FOREX Publication
Open Access | Rapid and quality publishing

International Journal of
Electrical and Electronics Research (IJEER)
Research Article | Volume 10, Issue 3 | Pages 765-771 | e-ISSN: 2347-470X

Performance Evaluation of Fuzzy One Cycle Control Based Custom Power Device for Harmonic Mitigation

Vasupalli Manoj[1], Dr. Prabodh Khampariya[2] and Dr. Ramana Pilla[3]

[1]Research Scholar, Department of Electrical Engineering, Sri Satya Sai University of Technology & Medical Sciences, Bhopal, India, manojv287@gmail.com

[2]Professor, Department of EEE, Sri Satya Sai University of Technology & Medical Sciences, Bhopal, India, khampariya5@gmail.com

[3]Professor, Department of EEE, GMR Institute of Technology, Rajam, India, ramana.pilla@gmrit.edu.in

***Correspondence:** Vasupalli Manoj & Dr. Ramana Pilla; manojv287@gmail.com, ramana.pilla@gmrit.edu.in

ABSTRACT- Custom power devices (CPDs) provide better harmonic minimization when they are connected in parallel with the distribution network. Power switches have a hard impact on harmonic production in distribution networks, which leads to aging effects. Techniques used to control CPD's provide full switching in various ways. A pulse width modulation (PWM) scheme requires a reference frame transformation that tracks source and load currents to produce a control signal. The voltage de-coupler is installed in the power device's current controllers to minimize fast current harmonics and remove complexity. One-cycle control (OCC) operates in dual boost converter mode and requires only source currents to produce a control signal. Minimum distortions are obtained by the output voltage feedback compensator. The proposed approach compares the performance of two methodologies based on total harmonic distortion (THD) analysis of the same grid voltage. The performance of the CPD using PI and fuzzy one-cycle control techniques is illustrated by simulation, which gives accurate results.

General Terms: Power Quality Improvement, Harmonic Distortions.

Keywords: Custom power device, one cycle control, Pulse width modulation, Fuzzy logic control, Total harmonic reduction.

ARTICLE INFORMATION

Author(s): Vasupalli Manoj, Dr. Prabodh Khampariya and Dr. Ramana Pilla

Received: 07/07/2022; **Accepted**: 29/09/2022; **Published**: 30/09/2022;

e-ISSN: 2347-470X;

Paper Id: IJEER 0707-03;

Citation: 10.37391/IJEER.100358

Webpage-link:
https://ijeer.forexjournal.co.in/archive/volume-10/ijeer-100358.html

crossref member CROSSREF.ORG THE CITATION LINKING BACKBONE

Publisher's Note: FOREX Publication stays neutral with regard to Jurisdictional claims in Published maps and institutional affiliations.

1. INTRODUCTION

In consideration of the expeditious evolution of the semiconductor industry, power electronic devices have acquired heyday in our day-to-day used house-hold electrical appliances. Moreover, these power electronic devices have gained gratuity in the electronics and electrical industry as they are the prominent source of power harmonics in the power distribution system. Power harmonics refers to the electric contamination on an electric distribution system that can be the origin of the power quality issues. So as to enhance the quality of power supply, there is a need of filtering process for these harmonics. In consequence, custom power device is considered to be a feasible substitute for power conditioning to dominance harmonic component in power system these days. Florescent lamp (namely arching loads), transformers (namely saturated devices) and power electronic devices will generate components of current and voltage with high frequencies among the power line. These high frequencies generated by the components of current and voltage are called as power harmonics. The harmonic disruptions in the power supply are triggered by the non-linear feature of the loads.

Adjustable Speed Drive (ASD) and variable frequency drives (VFD) are the applications which have high penetration to distribution network [1][2]. A Series active power filter is proposed to compensate load voltage harmonics but it requires voltage control loop to develop a control signal in addition [3]. Continuously adapted harmonics cancellation (CAHC) method is used to regulate the clocked system disturbances [4]. A LCL type STATCOM with decoupled configuration is designed to reduce the internal and external disturbances in the distribution system [5][6]. Fuzzy neural network controller is implemented to reduce the total harmonic distortion due to nonlinear load changing [7].

Sliding mode controller based three phase custom power devices with two legs is introduced to reduce the source current harmonics and to reduce the switching losses [8]. Solar cell fed custom power device is utilized to mitigate harmonics which is effect for low source cost [9]. Online learning control with PWM pulse generation is discussed to regulate current harmonics [10]. A trap LCL filter is placed at the load side to compensate harmonic currents due to nonlinear loads which are connected to grid [11][12]. To extract the fundamental components in the voltage wave for a shunt active power filter Kalman filters are used as a sensor less vector control [13]. A multilevel inverter based active power filter is developed with an open-end winding transformer used to reduce harmonic currents [14].
Hybrid active power filter is used as variable harmonic conductance to reduce distortions [15]. Novel control logic for

International Journal of
Electrical and Electronics Research (IJEER)
Open Access | Rapid and quality publishing
Research Article | Volume 10, Issue 3 | Pages 765-771 | e-ISSN: 2347-470X

the active filter, based on a virtual resistor injection to compensate AC side harmonics [16]. An active damping mechanism is reviewed to mitigate harmonic frequencies up to a better extend [17]. Low-cost shunt passive filter is designed for power factor improvement. The effect of resonance problem is reduced [18]. Band less hysteresis technique with neural network control is proposed to limit the harmonic currents [19]. OCC control tracks only source currents and no need of reference frame transformation [20]. Voltage decoupler method is used to compensate current harmonics to provide active current harmonic reduction and simplify the control logic [21]. In this paper, A PWM based custom power device with voltage decoupler for current controller is proposed to operate under nonlinear load conditions. Voltage detector is used additionally when compared with the conventional method for smooth current extraction. Also, a one cycle control approach is proposed; which operates under dual boost converter mode. The OCC is effective and faster harmonic current limiter with low switching losses. At each 60^0 of operation one of the phases will be in positive or negative cycle. Based on the operating conditions custom power device is operated as parallel connected dual boost converter. The two methods such as, PWM and OCC techniques are compared for the same base system. Total harmonic distortion (THD) of each method is validated using MATLAB/Simulink.

2. SHUNT CONNECTED CUSTOM POWER DEVICE

Figure 1 depicts the block diagram of a shunt connected custom power device. It is the closed loop system used for harmonic reduction. The custom power device will inject the compensating current. If to the power system based on the load changes. The source current, I_s is obtained using the equation.

$$I_s = I_f + I_L \tag{1}$$

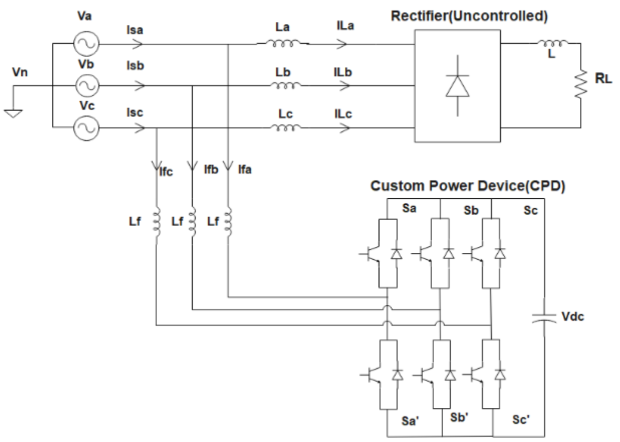

Figure 1: Basic principle of harmonic currents compensations

3. PWM CONTROL OF CUSTOM POWER DEVICE

The main objective of a custom power device is to produce compensating currents into the distribution network. The compensating current produced is of equal and opposite to the harmonic current in the line. This will result in sinusoidal source current in the power system.

3.1 Normal or Body Text

Figure 2 presents the PWM based control approach. Voltage across the capacitor, filter currents and load currents are taken as feedback. By using Park's transformation load currents and filter currents are converted into two phases.

$$\begin{bmatrix} i_d \\ i_q \\ i_0 \end{bmatrix} = \frac{2}{3}\begin{bmatrix} \sin\theta & \sin(\theta-120^0) & \sin(\theta+120^0) \\ \cos\theta & \cos(\theta-120^0) & \cos(\theta+120^0) \\ 1/2 & 1/2 & 1/2 \end{bmatrix}\begin{bmatrix} i_a \\ i_b \\ i_c \end{bmatrix} \tag{2}$$

The load currents i_{dl} & i_{ql} are passed through low pass filter which produces fundamental currents 'i_1'. To generate total harmonic current i_1 is compared with i_{dl}.

$$i_{df} = i_1 - i_{dL} \tag{3}$$

DC link voltage is observed using voltage detector and is compared with a reference voltage to produce current command signal.

$$\mathrm{I_m} = G(s)\left(V_{dc}^* - V_{dc}\right) \tag{4}$$

Here, G(s) is dc voltage regulator which consists of proportional integral controller (PI). To minimize the capacitor voltage fluctuations and to develop proportional current magnitude PI controller is utilized. Current command signal I_m is added to total harmonic current I_{df}^* to develop the current magnitude.

$$i_{df} = i_1 - i_{dL} + \mathrm{I_m} \tag{5}$$

$$i_{qf} = -i_{qf} \tag{6}$$

Filter currents are compared with harmonic currents to produce the error. The error is given to the current controller to produce necessary reference voltages.

$$V_{df} = \left[K_p + \frac{K_i}{s}\right]\left[i_{df}^* - i_{df}\right] \tag{7}$$

$$V_{qf} = \left[K_p + \frac{K_i}{s}\right]\left[i_{qf}^* - i_{qf}\right] \tag{8}$$

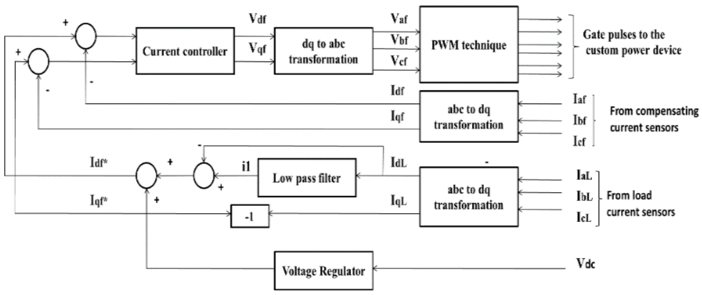

Figure 2: Block diagram of PWM controller custom power device

FOREX Publication
Open Access | Rapid and quality publishing

International Journal of
Electrical and Electronics Research (IJEER)
Research Article | Volume 10, Issue 3 | Pages 765-771 | e-ISSN: 2347-470X

4. ONE CYCLE CONTROL OF CUSTOM POWER DEVICE

A three-phase shunt custom power device is made up of a voltage source converter (VSC) and a three-phase nonlinear load linked in shunt. Controlling VSC with only source current sensors is preferable than one cycle control. One cycle of measured source voltage signal is divided into 6 regions. Two of the voltages in each zone are either positive or negative, and the third is the polar opposite. For every 60^0 the custom power device is operated as a dual boost converter as shown in *figure 3*.

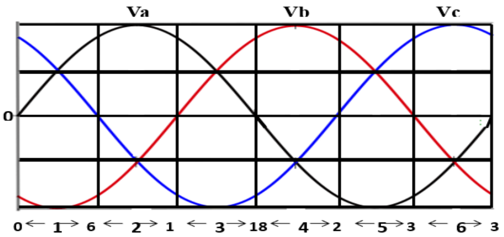

Figure 3: Three phase source voltage waveforms with region selector

4.1 Custom Power Device as dual boost converter

For, first (0-60^0) region the phase voltage V_b holds the negative value. The switches in the middle limb are operated in which S_b is switched OFF & S_b' is switched ON. *Figure 4* shows the outcome of changing a voltage source converter to a dual boost converter with two grid voltages, V_{ab} and V_{cb}. V_{ab}, V_{cb} are line-to-line voltages and V_{dc} is the capacitor across voltage that acts as an energy storage.

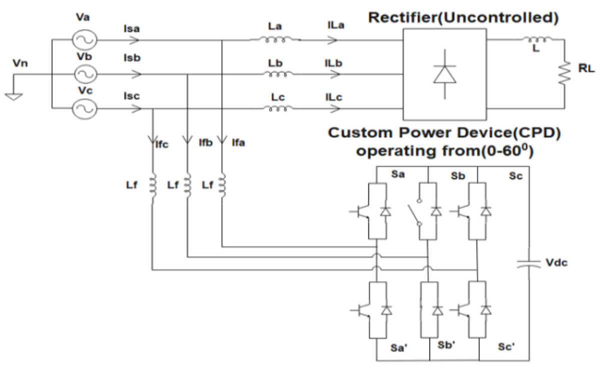

Figure 4: Power stage of the custom power device

Let V_{ab}=V_p and V_{cb}=V_n based on voltage relationship the equivalent circuit of the dual boost converter for (0-60^0) is

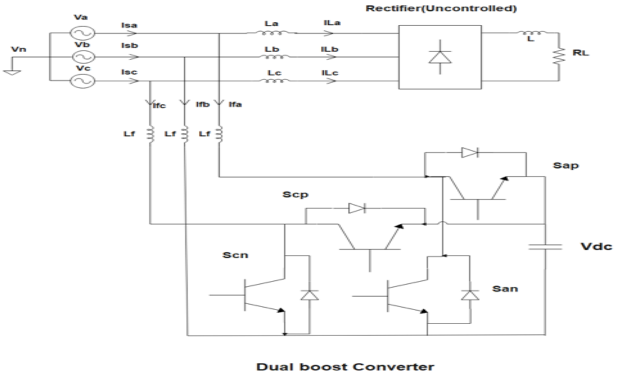

Figure 5: The equivalent dual-boost converter

$$\begin{bmatrix} V_p^* \\ V_n^* \\ V_t^* \end{bmatrix} = \begin{bmatrix} 2/3 & -1/3 \\ -1/3 & 2/3 \\ 1/3 & 1/3 \end{bmatrix} \begin{bmatrix} V_p \\ V_n \end{bmatrix} \quad (9)$$

The above equation is developed using source inductor voltages at dual boost converter mode. Based on voltage analysis, voltage across each inductor is illustrated during each switching state in *table-1*.

Table 1: Switching states

State	V_p	V_n	$\bar{V}_p$	$\bar{V}_n$	V_{Lp}	V_{Ln}	V_{Lt}
I	ON	ON	OFF	OFF	Vp*	Vn*	Vt*
II	ON	OFF	OFF	ON	Vp*+1/3×Vdc	Vn*-2/3 ×Vdc	Vt*-1/3×Vdc
III	OFF	ON	ON	OFF	Vp*-2/3×Vdc	Vn*+1/3×Vdc	Vt*-1/3×Vdc
IV	OFF	OFF	ON	ON	Vp*-1/3×Vdc	Vn*-1/3×Vdc	Vt*-2/3×Vdc

From the above table the switching sequence is possible for I, II, III, IV states. By assuming switching frequency is higher than the fundamental frequency. The generated equations based on duty ratio are:

$$V_p^*Q_n + \left(V_p^* + \tfrac{1}{3}V_{dc}\right)\times(Q_p - Q_n) + \left(V_p^* - \tfrac{1}{3}V_{dc}\right)\times(1 - Q_p) = 0 \quad (10)$$

$$V_n^*Q_n + \left(V_n^* - \tfrac{2}{3}V_{dc}\right)\times(Q_p - Q_n) + \left(V_n^* - \tfrac{1}{3}V_{dc}\right)\times(1 - V_p) = 0 \quad (11)$$

$$V_t^*Q_n + \left(V_t^* - \tfrac{1}{3}V_{dc}\right)\times(Q_p - Q_n) + \left(V_t^* - \tfrac{2}{3}V_{dc}\right)\times(1 - Q_p) = 0 \quad (12)$$

The following equations are true for three phase symmetrical system

$$V_p^* + V_n^* - V_t^* = 0 \quad (13)$$

Replacing V_t^* in terms of V_p^* *and* V_n^* the above equation can be simplified as

$$\begin{bmatrix} 1-Q_p \\ 1-Q_n \end{bmatrix} = \begin{bmatrix} 2 & 1 \\ 1 & 2 \end{bmatrix} \begin{bmatrix} V_p^* \\ V_n^* \end{bmatrix} \quad (14)$$

The above equation gives an inherent relationship between the duty cycle and the input, output voltage for the dual-boost converter.

4.2 One Cycle Control Approach for Three Phase Custom Power Device

One-cycle control provides the required compensating harmonic signals to make source currents sinusoidal. The relation between source current and voltage depends on emulated resistance and is given by

$$V_a = R_e\, i_a, V_b = R_e\, i_b, V_c = R_e\, i_c \quad (15)$$

Where R_e is emulated resistance which is used to control the equivalent currents i_p and i_n. The above equation can be rewritten as

$$V_p^* = R_e\, i_p, V_n^* = R_e\, i_n \quad (16)$$

On substituting *eq. 15 & 16* in *eq. 14*, we have

$$\begin{bmatrix} 1-Q_p \\ 1-Q_n \end{bmatrix} = \frac{R_e}{V_{dc}R_s}\times R_s \begin{bmatrix} 2 & 1 \\ 1 & 2 \end{bmatrix} \begin{bmatrix} i_p \\ i_n \end{bmatrix} \quad (17)$$

FOREX Publication
Open Access | Rapid and quality publishing
International Journal of
Electrical and Electronics Research (IJEER)
Research Article | Volume 10, Issue 3 | Pages 765-771 | e-ISSN: 2347-470X

Let $V_m = \frac{V_{dc} \times R_s}{Re}$, is the control signal generated by using PI controller. The above eqn. can be written as

$$V_m \begin{bmatrix} 1-Q_p \\ 1-Q_n \end{bmatrix} = R_s \begin{bmatrix} 2 & 1 \\ 1 & 2 \end{bmatrix} \begin{bmatrix} i_p \\ i_n \end{bmatrix} \quad (18)$$

The control mode of operation is obtained by varying the duty ratio shown in *figure 6*.

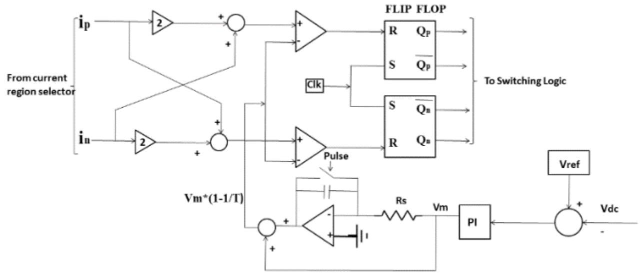

Figure 6: One cycle control (OCC) for control pulse generation

5. TOPOLOGICAL COMPARISION

The suggested OCC-based CPD outperforms both the traditional OCC and PWM approach. *Table 2* summarizes the requirements of several methods for easy comparison with other existing harmonic correction strategies. From *table 2* it is clear that, when compared to other schemes, OCC-based systems are simple to construct without a PLL. All other designs necessitate a greater number of sensors than most OCC schemes. They also require high-bandwidth current controllers that are specifically built for them. Due to the nonlinear property of its current controller, the OCC system integrates the current controller with the PWM modulator and has a fast dynamic response. In comparison to standard OCC, the suggested OCC methodology in the paper only requires three additional sensors, as well as only two flip flops for pulse production. The harmonic performance of this control method is satisfactory.

Table 2: Comparison between conventional and proposed methods

Controller	Sensors (Current Amps)	Control Signal generation	Pulse generation	PLL	No. of sensors
PWM Control Conventional Method	Required source, load current sensors and source voltage sensors	Parks transformation	10kHZ	Yes	10
PWM Control Proposed Method	Required source, compensating current sensors and source voltage sensors	Parks transformation	12.5kHZ	Yes	10
One Cycle Control Conventional Method	Required source current and voltage sensors	Region Selector	12.8kHz	No	7
One Cycle Control Proposed Method	Required source current and voltage sensors	Region Selector	13kHz	No	7

6. FUZZY LOGIC CONTROLLER

Increasing success has come from using the underlying concepts of observation as part of a Fuzzy control framework. To enhance performance, fuzzy frameworks are often updated to incorporate additional criteria or features. Fuzzy control may be used to enhance traditional control architectures by providing more knowledge beyond what is already available. The Fuzzy Inference System Editor is part of the controller's fuzzy logic. This FIS editorial manager recreates a sophisticated exchange circuit. The fuzzy controller adds V_{Cr} and I_{Cr} to the system. The value generated by the controller is brand new. There are several different editors available inside this graphical user interface, including a membership work editor, FIS editor, rule editor, surface viewer, and rule viewer.

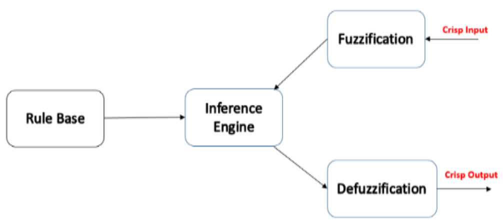

Figure 7: Fuzzy inference system

6. SIMULATION RESULTS

Table 4: Test system data

Three-Phase Source	RMS Voltage (Vrms) = 120V Supply Frequency (f) = 60 HZ Source inductance (Ls) = 0.4 mH
Nonlinear Load (balanced)	Bridge Rectifier with L_0= 3.1 mH, R_0 = 8.67Ω, C_0 =3300 µF
Custom power device specifications	Inductance(L_2) = 0.25mH, Input Resistance(R_2) = 0.03 Ω, DC link capacitor = 4800 µF.
DC-Link Capacitor	Voltage (V_C) = 400V.

The proposed PI OCC and Fuzzy OCC methods are validated under a variety of load scenarios through simulation.

7.1 Without Custom Power Device (CPD)

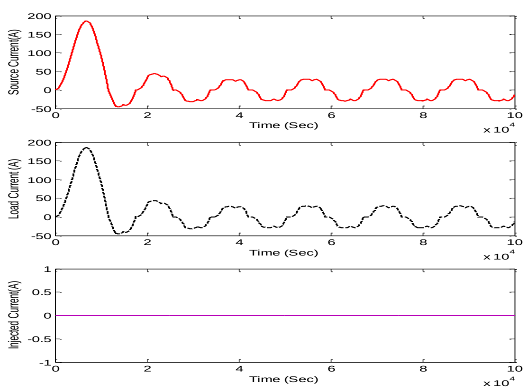

Figure 8: Simulation results of Non- Linear Load (a) Source Current (b) Load Current (c) Injected Current

FOREX Publication
Open Access | Rapid and quality publishing
International Journal of
Electrical and Electronics Research (IJEER)
Research Article | Volume 10, Issue 3 | Pages 765-771 | e-ISSN: 2347-470X

Figure 8 (a) shows that the source current does not have a sinusoidal waveform because of the nonlinear load. In *figure 8* (b) and *figure 8 (c)*, we can see the load current and the injected current.

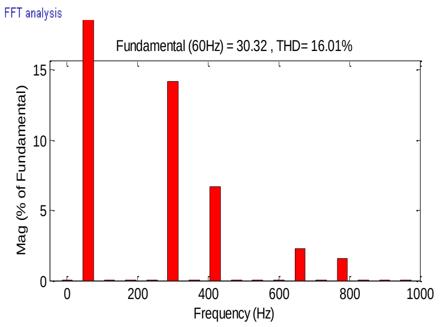

Figure 9: THD of Source Current

From FFT analysis THD of Source Current is 16.01%.

7.2 Custom Power Device (CPD) with OCC PI Controller

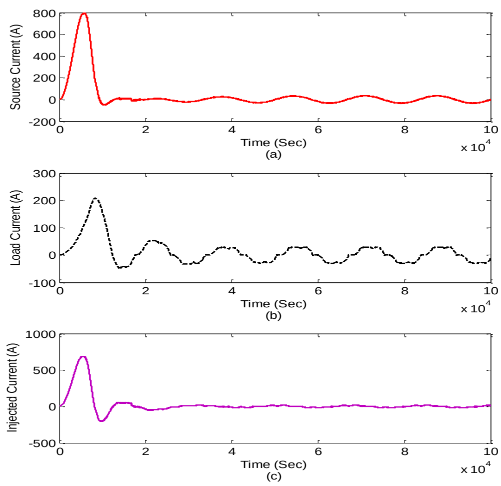

Figure 10: Simulation results with APF (a) Source Current (b) Load Current (c) Injected Current

The CPD causes the source current to have a sinusoidal waveform, as seen in *figure 10 (a).* The load and injected currents are shown in *figure 10 (b)& 10(c).* From FFT analysis THD of source current is 3.40%

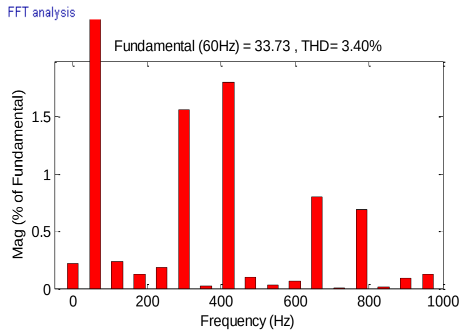

Figure 11: THD of Source Current

7.3 Custom Power Device (CPD) with OCC Fuzzy Controller

If one examines *figure 13*, they will see that the source current waveform is sinusoidal because of SAPF. *Figure 12(b) and 12(c)* depict the load current and injecting current, respectively.

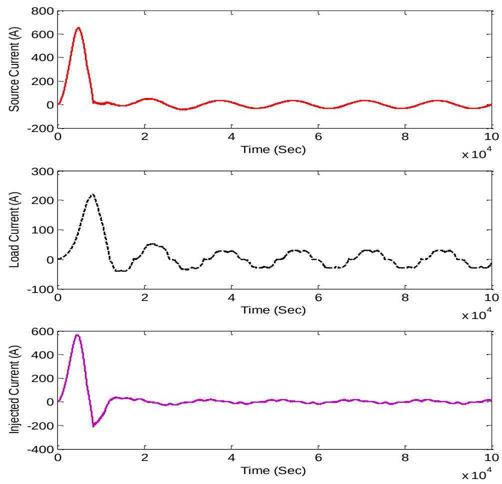

Figure 12: Simulation results with APF (a) Source Current (b) Load Current (c) Injected Current

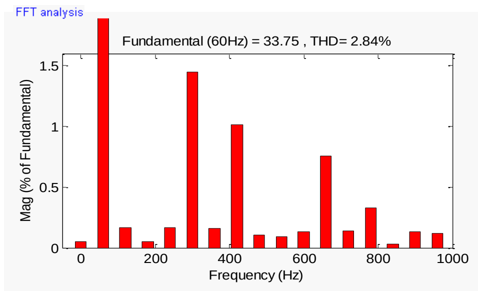

Figure 13: THD of Source Current

From FFT analysis THD of Source Current is 2.84%.

7.4 PWM OCC Controller with Combination of Balanced Load

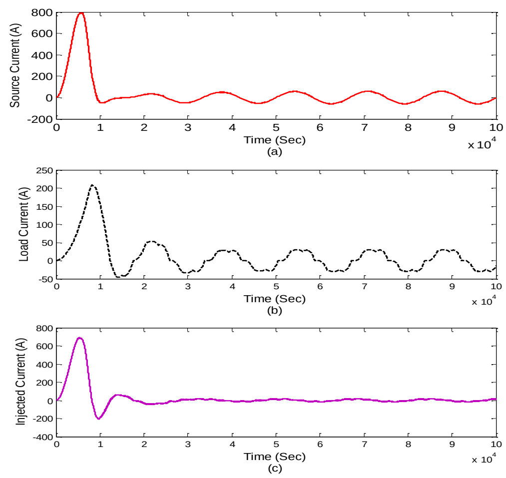

Figure 14: Simulation results with PI with combination of Unbalanced Load (a) Source Current (b) Load Current (c) Injected Current

FOREX Publication
Open Access | Rapid and quality publishing

International Journal of
Electrical and Electronics Research (IJEER)
Research Article | Volume 10, Issue 3 | Pages 765-771 | e-ISSN: 2347-470X

The CPD causes the source current to have a sinusoidal waveform, as seen in *figure 14 (a).* The load and Injected currents are shown in *figure 14(b)&14 (c).*

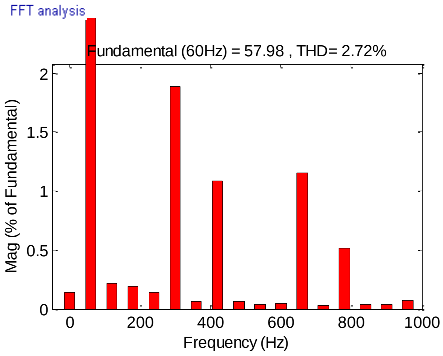

Figure 15: THD of Source Current

From FFT analysis THD of source current is 2.72%.

7.5 Fuzzy OCC Controller with Combination of Balance Load

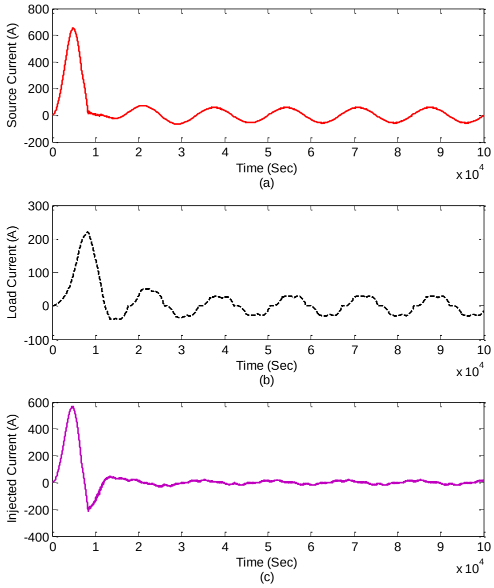

Figure 16: Simulation results with FUZZY with Balanced Highly Inductive Load (a) Source Current (b) Load Current (c) Injected Current

The CPD causes the source current to have a sinusoidal waveform, as seen in *figure 16 (a).* The load current and injected current are equal, as shown in *figure 16 (b) &16(c).*

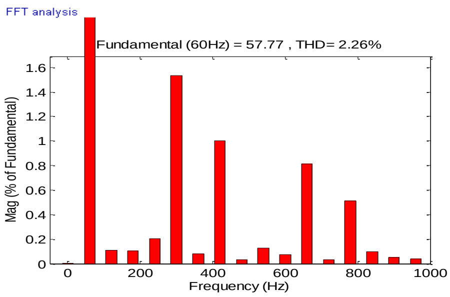

Figure 20: THD of Source Current

From FFT analysis THD of Source Current is 2.26%.

Table 5: Load values for both PI OCC and Fuzzy OCC techniques

Type of Load	Load	Load value
Unbalanced Load	Resistance	15Ω, 6Ω, 8Ω
	Inductance	8e-3H, 4e-3H
Balanced Load	Resistance	7Ω
	Inductance	10H

Table 6: Simulation test results of distribution system under nonlinear loading

Operating Conditions	% THD with PI OCC controller	% THD with FUZZY OCC controller
Without CPD	16.01	16.01
With CPD	3.40	2.84
CPD with Combination of Unbalanced load	3.39	3.12
CPD with Combination of Unbalanced and Balanced load	2.64	2.62
CPD with Combination of Balanced load	2.72	2.26
CPD with Combination of Balanced Highly Inductive load	3.40	2.82
CPD with Combination of Balanced Highly Inductive load and Unbalanced load	3.37	3.07

From *table 6*, the THD of source current is same for both PI controller technique and fuzzy controller technique when the active power filter is not connected to the system. It can also be seen that there are lower THD values of source current when Active Power Filter (APF) with fuzzy controller is connected to the system when compared to the THD values of source current when APF with PI controller is connected to the system.

8. CONCLUSION

In this research work, current distortion due to nonlinear loads and compensation with various methods is presented. The proposed PI OCC and Fuzzy OCC schemes for shunt CPD are used to compensate the source current harmonics. With custom power device connected to nonlinear load, it is observed that with conventional OCC method the harmonic distortion is reduced to 3.40% while in the proposed fuzzy OCC technique Harmonic distortion is 2.84%. Hence, by increasing the switching frequency and adding voltage decoupler the harmonic distortions are reduced to a good extent. On the other hand, one cycle control scheme requires less sensors, so the cost of design is less when compared to PWM technique. Conventional OCC technique requires more flip flops for pulse generation while the proposed OCC method requires only two Flip flops, and the additional advantage is it does not require PLL. It is observed that, by using conventional OCC method, the total harmonic distortion is reduced to 2.72% and by using proposed fuzzy OCC method the harmonic distortion is minimized to 2.26% for balanced loads. This research reveals that it is more economical and reliable to use the proposed OCC technique based custom power device for harmonic reduction for various loads to evaluate the performance of distribution system.

9. ACKNOWLEDGMENTS
The authors would like to express their gratitude to the management of Sri Satya Sai University of Technology & Medical Sciences and GMR Institute of Technology for providing the essential resources and facilities for completion of the research work.

REFERENCES
[1] A. Alduraibi, J. Yaghoobi, D. Solatialkaran, and F. Zare, “A Modular Power Converter with Active Front-End System to Mitigate Harmonics in Distribution Networks,” IEEE J. Emerg. Sel. Top. Power Electron., vol. 9, no. 2, pp. 1725–1735, Apr. 2021, doi: 10.1109/JESTPE.2020.2993786.

[2] R. Pandurangan, P. Kaliannan, and P. Shanmugam, “Effects of Current Distortion on DC Link Inductor and Capacitor Lifetime in Variable Frequency Drive Connected to Grid with Active Harmonic Filter,” IEEE Trans. Ind. Appl., vol. 57, no. 1, pp. 492–505, Jan. 2021, doi: 10.1109/TIA.2020.3028555.

[3] L. F. J. Meloni, F. L. Tofoli, A. J. J. Rezek, and E. R. Ribeiro, “Modeling and Experimental Validation of a Single-Phase Series Active Power Filter for Harmonic Volt age Reduction,” IEEE Access, vol. 7, pp. 151971–151984, 2019, doi: 10.1109/ACCESS.2019.2947917.

[4] A. Bendicks, T. Dörlemann, S. Frei, N. Hees, and M. Wiegand, “Active EMI Reduction of Stationary Clocked Systems by Adapted Harmonics Cancellation,” IEEE Trans. Electromagn. Compat., vol. 61, no. 4, pp. 998–1006, Aug. 2019, doi: 10.1109/TEMC.2018.2854965.

[5] M. Wang, X. Wang, J. Qiao, and L. Wang, “Improved Current Decoupling Method for Robustness Improvement of LCL-type STATCOM Based on Active Disturbance Rejection Control,” IEEE Access, vol. 7, pp. 121781–121792, 2019, doi: 10.1109/ACCESS.2019.2931747.

[6] L. Wang, X. Han, C. Ren, Y. Yang, and P. Wang, “A Modified One-Cycle-Control-Based Active Power Filter for Harmonic Compensation,” IEEE Trans. Ind. Electron., vol. 65, no. 1, pp. 738–748, Jan. 2018, doi: 10.1109/TIE.2017.2682021.

[7] K. H. Tan, F. J. Lin, and J. H. Chen, “DC-Link voltage regulation using RPFNN-AMF for Three-Phase active power filter,” IEEE Access, vol. 6, pp. 37454–37463, Jun. 2018, doi: 10.1109/ACCESS.2018.2851250.

[8] J. Morales, L. G. De Vicuna, R. Guzman, M. Castilla, and J. Miret, “Modeling and Sliding Mode Control for Three-Phase Active Power Filters Using the Vector Operation Technique,” IEEE Trans. Ind. Electron., vol. 65, no. 9, pp. 6828–6838, Sep. 2018, doi: 10.1109/TIE.2018.2795528.

[9] S. Kumar and B. Singh, “A Multipurpose PV System Integrated to a Three-Phase Distribution System Using an LWDF-Based Approach,” IEEE Trans. Power Electron., vol. 33, no. 1, pp. 739–748, Jan. 2018, doi: 10.1109/TPEL.2017.2665526.

[10] N. Malla, U. Tamrakar, D. Shrestha, Z. Ni, and R. Tonkoski, “Online learning control for harmonics reduction based on current controlled voltage source power inverters,” IEEE/CAA J. Autom. Sin., vol. 4, no. 3, pp. 447–457, Jul. 2017, doi: 10.1109/JAS.2017.7510541.

[11] J. Fang, X. Li, X. Yang, and Y. Tang, “An Integrated Trap-LCL Filter with Reduced Current Harmonics for Grid-Connected Converters under Weak Grid Conditions,” IEEE Trans. Power Electron., vol. 32, no. 11, pp. 8446–8457, Nov. 2017, doi: 10.1109/TPEL.2017.2651152.

[12] C. S. Lam, L. Wang, S. I. Ho, and M. C. Wong, “Adaptive Thyristor-Controlled LC-Hybrid Active Power Filter for Reactive Power and Current Harmonics Compensation with Switching Loss Reduction,” IEEE Trans. Power Electron., vol. 32, no. 10, pp. 7577–7590, Oct. 2017, doi: 10.1109/TPEL.2016.2640304.

[13] R. Guzman, L. G. De Vicuna, J. Morales, M. Castilla, and J. Miret, “Model-Based Control for a Three-Phase Shunt Active Power Filter,” IEEE Trans. Ind. Electron., vol. 63, no. 7, pp. 3998–4007, Jul. 2016, doi: 10.1109/TIE.2016.2540580.

[14] G. A. De Almeida Carlos, C. B. Jacobina, E. C. Dos Santos, E. L. L. Fabrício, and N. Rocha, “Shunt Active Power Filter With Open-End Winding Transformer and Series-Connected Converters,” IEEE Trans. Ind. Appl., vol. 51, no. 4, pp. 3273–3283, Jul. 2015, doi: 10.1109/TIA.2015.2394318.

[15] T. L. Lee, Y. C. Wang, J. C. Li, and J. M. Guerrero, “Hybrid active filter with variable conductance for harmonic resonance suppression in industrial power systems,” IEEE Trans. Ind. Electron., vol. 62, no. 2, pp. 746–756, Feb. 2015, doi: 10.1109/TIE.2014.2347008.

[16] S. Bai and S. M. Lukic, “Unified active filter and energy storage system for an MW electric vehicle charging station,” IEEE Trans. Power Electron., vol. 28, no. 12, pp. 5793–5803, 2013, doi: 10.1109/TPEL.2013.2245146.

[17] J. Dannehl, M. Liserre, and F. W. Fuchs, “Filter-based active damping of voltage source converters with LCL filter,” IEEE Trans. Ind. Electron., vol. 58, no. 8, pp. 3623–3633, Aug. 2011, doi: 10.1109/TIE.2010.2081952.

[18] A. Hamadi, S. Rahmani, and K. Al-Haddad, “A hybrid passive filter configuration for VAR control and harmonic compensation,” IEEE Trans. Ind. Electron., vol. 57, no. 7, pp. 2419–2434, Jul. 2010, doi: 10.1109/TIE.2009.2035460.

[19] M. A. M. Radzi and N. A. Rahim, “Neural network and bandless hysteresis approach to control switched capacitor active power filter for reduction of harmonics,” IEEE Trans. Ind. Electron., vol. 56, no. 5, pp. 1477–1484, 2009, doi: 10.1109/TIE.2009.2013750.

[20] C. Qiao, T. Jin, and K. M. Smedley, “One-cycle control of three-phase active power filter with vector operation,” IEEE Trans. Ind. Electron., vol. 51, no. 2, pp. 455–463, Apr. 2004, doi: 10.1109/TIE.2004.825223.

[21] H.-H. Kuo, S.-N. Yeh, and J.-C. Hwang, “Novel analytical model for design and implementation of three-phase active power filter controller”, doi: 10.1049/ipepa:20010433.

[22] Sandhya Kulkarni and Archana Thosar (2022), Performance Analysis of Fault Tolerant Operation of PMSM using Direct Torque Control and Fuzzy Logic Control. IJEER 10(2), 297-307. DOI: 10.37391/IJEER.100240.

[23] M Rupesh, Dr. T S Vishwanath (2021), Fuzzy and ANFIS Controllers to Improve the Power Quality of Grid Connected PV System with Cascaded Multilevel Inverter. IJEER 9(4), 89-96. DOI: 10.37391/IJEER.090401.

[24] Ganiyu Adedayo Ajenikoko, Ridwan Abiola Oladepo (2018), Impact of System Average Interruption Duration Index Threshold on the Reliability Assessment of Electrical Power Distribution Systems. IJEER 6(2), 17-31. DOI: 10.37391/IJEER.060203. http://ijeer.forexjournal.co.in/papers-pdf/ijeer-060203.pdf

[25] Prof. Kalyani Kurundkar and Dr. G. A. Vaidya (2021), Application of HFPSO-TOPSIS approach for optimally locating and sizing of reactive power compensating devices for voltage control ancillary service. IJEER 9(3), 16-26. DOI: 10.37391/IJEER.090301. https://ijeer.forexjournal.co.in/archive/volume-9/ijeer-090301.html